

# How Sampling Impacts the Robustness of Stochastic Neural Networks

Sina Däubener                      Asja Fischer  
Faculty of Computer Science, Ruhr University Bochum

## Abstract

Stochastic neural networks (SNNs) are random functions and predictions are gained by averaging over multiple realizations of this random function. Consequently, an adversarial attack is calculated based on one set of samples and applied to the prediction defined by another set of samples. In this paper we analyze robustness in this setting by deriving a sufficient condition for the given prediction process to be robust against the calculated attack. This allows us to identify the factors that lead to an increased robustness of SNNs and helps to explain the impact of the variance and the amount of samples. Among other things, our theoretical analysis gives insights into (i) why increasing the amount of samples drawn for the estimation of adversarial examples increases the attack’s strength, (ii) why decreasing sample size during inference hardly influences the robustness, and (iii) why a higher prediction variance between realizations relates to a higher robustness. We verify the validity of our theoretical findings by an extensive empirical analysis.

## 1 Introduction

Since the discovery of adversarial examples [Biggio et al., 2013, Szegedy et al., 2014], many works were dedicated to hinder attacks [e.g. Madry et al., 2018, Papernot et al., 2016] or to enhance attack strategies [e.g. Athalye et al., 2018, Akhtar and Mian, 2018, Carlini and Wagner, 2017b, Uesato et al., 2018]. However, due to the high dimensional properties of deep neural networks (DNNs) it has been shown that practical adversarial attacks can not in general be ruled out [e.g. Ilyas et al., 2019].

Therefore, another line of research focuses on formulating robustness guarantees for DNNs. These often specify the radius of a ball around input points in which perturbations do not lead to a label change [Hein and Andriushchenko, 2017]. The maximal radius corresponds to the distance of the input point to the nearest decision boundary, which on the other hand is equal to the length of the smallest perturbation vector that leads to a misclassification. Such a robustness analysis assumes that the decision boundaries are fixed and that the attacker is able to estimate (at least approximately) the direction of this minimal perturbation vector, which is a reasonable assumption for deterministic networks but usually does not hold for stochastic neural networks (SNNs).

Stochastic neural networks, and stochastic classifiers more generally, are random functions and predictions are given by the expectation of the value of the random function for the given input. In practice this expectation is usually not tractable, and hence it is approximated by averaging over multiple realizations of the random function. This approximation leads to the challenging setting, where predictions, decision boundaries, and gradients become random variables themselves. Hence, under an adversarial attack the decision boundaries used for calculating the attack and those used when predicting the label for the resulting attack differ. This means that the attacker can not estimate the optimal perturbation direction - even when the attack is based on (infinitely) many samples as for example proposed by Athalye et al. [2018] - which leads to an increase of robustness in practice. In this paper we study how robustness of SNNs arises from this misalignment of the attack direction and the optimal perturbation direction during inference that results from the stochasticity. First, we derive a sufficient condition for a SNN prediction relying on one set of samples to be robust wrt. an attack that was calculated on a second set of samples. Then, we conduct an analysis on the factors influencing this robustness, which leads to new insights on how the amount of samples during attack estimation and inference as well as the prediction variance impact the robustness of the SNN. Moreover, the analysis contributes to the understanding why stochastic nets are more robust than deterministic ones. Lastly, we conduct an empirical analysis that demonstrates that the novel insights perfectly match what we observe in practice.

## 2 Related work

Many works proposed to include stochasticity into their network to increase the robustness which they demonstrated empirically [e.g. Raff et al., 2019, Xie et al., 2018, He et al., 2019]. Their motivation for doing so ranges from increasing the smoothness of decision boundaries [Addepalli et al., 2021], over decreasing the sensitivity to changes in the input [Bender et al., 2020] to gradient masking [Dhillon et al., 2018]. As discussed by Athalye

et al. [2018], gradient masking due to stochastic gradients can result in overestimating robustness, if attacks are based on only a single gradient sample. They thus propose taking multiple samples as adequate defense strategy.

Another line of research focuses on certified or provable robustness [e.g. Carlini et al., 2018, Katz et al., 2017, Wong and Kolter, 2018]. Hein and Andriushchenko [2017] investigated robustness as the guarantee that the label will not change within an  $\epsilon$ -region around the input. They developed a regularization based training method which leads to such robustness guarantees for specific  $L_p$ -attacks. In subsequent work [Croce et al., 2019, Croce and Hein, 2020] this approach was further refined to account for ReLU networks and general  $L_p$ -norms.

Meanwhile, Lécuyer et al. [2019] derived robustness guarantees in an  $\epsilon$ -region for arbitrary model types by incorporating one noise layer during training. Cohen et al. [2019] further proved a tighter robustness guarantee by applying randomized smoothing.

Recent works focus on analyzing and increasing the robustness of ensembles of neural networks [Dabouei et al., 2020, Yang et al., 2022], where the diversity of the single deterministic networks (and their gradients) were found to be an important robustness factor.

Another line of research analyzes the robustness of Bayesian Neural Networks (BNNs). Wicker et al. [2020] certified robustness of BNNs by estimating the probability for the network to project points from a region around the input into the same output region based on interval bound propagation. The same methodology was used to derive guarantees for the robustness of BNNs with modified adversarial training [Wicker et al., 2021]. Moreover, Carbone et al. [2020] investigate robustness in the infinite-width infinite-sample limit.

To the best of our knowledge, no existing theoretical analysis of stochastic networks explicitly took into account the fact that realizations of SNN used during attack and inference differ.

### 3 Theoretical robustness analysis

We start our analyses with formalizing stochastic classifiers and adversarial attacks, before we derive conditions for stochastic classifiers to be robust under a stochastic attack and conduct our robustness analysis.

#### 3.1 Stochastic classifiers

We use the term *stochastic classifiers* for all classifiers which have an inherent stochasticity through the use of random variables in the model.

**Definition 3.1** (Stochastic classifiers). A stochastic classifier of  $k$ -classes corresponds to a function  $f : \mathbb{R}^d \times \Omega^h \rightarrow \mathbb{R}^k$ , mapping a pair  $(x, \Theta)$  of a given input point  $x \in \mathbb{R}^d$  and a random vector  $\Theta \in \Omega^h$  with probability distribution  $p(\Theta)$  to  $f(x, \Theta) = (f_1(x, \Theta), \dots, f_k(x, \Theta))^T$ , where  $f_c(x, \Theta)$  for  $c = 1, \dots, k$  is the discriminant function corresponding to the  $c$ -th class. The prediction of a stochastic classifier is given by  $f(x, \Theta) = \mathbb{E}_{p(\Theta)}[f(x, \Theta)]$  and the predicted class by

$$\arg \max_c \mathbb{E}_{p(\Theta)}[f_c(x, \Theta)] . \quad (1)$$

Under this generic definition of stochastic classifiers we find linear models with random weights, but also more complicated methods like Bayesian neural networks [Neal, 1996], infinite mixtures [Däubener and Fischer, 2020], Monte Carlo dropout networks [Gal and Ghahramani, 2016] or other types of neural networks which use stochasticity at input level [e.g. Cohen et al., 2019, Lécuyer et al., 2019, Raff et al., 2019], or during a forward pass like for example in parametric noise injection [He et al., 2019].

In cases where  $f(x, \Theta) = \mathbb{E}_{p(\Theta)}[f(x, \Theta)]$  is not tractable — which is usually the case in practice — the prediction of the stochastic classifier is approximated by its Monte Carlo (MC) estimate

$$f^{\mathcal{S}}(x) := \frac{1}{S} \sum_{s=1}^S f(x, \theta_s) , \quad (2)$$

where the sample set  $\mathcal{S} = \{\theta_1, \dots, \theta_S\}$  is drawn from  $p(\Theta)$ . Note, that  $f^{\mathcal{S}}$  is an unbiased estimate of the true predictive distribution  $f$  and according to the central limit theorem (CLT) its variance depends on the variance of  $f(x, \theta_i)$ . More precisely, since  $f(x, \theta_i)$  represents a random variable with mean  $f(x, \Theta)$  and some covariance  $\Sigma$  the CLT states that  $\sqrt{S}(f^{\mathcal{S}}(x) - f(x, \Theta)) \rightarrow \mathcal{N}(0, \Sigma)$ , and thus for sufficiently large sample size  $S$  approximately  $f^{\mathcal{S}}(x) \sim \mathcal{N}(f(x, \Theta), \frac{1}{S}\Sigma)$ .

#### 3.2 Adversarial attacks on stochastic classifiers

Let there be a given sample  $x$ , with corresponding label  $y \in [1, \dots, k]$ , that is classified correctly by a multi-class classifier  $f(\cdot) = (f_1(\cdot), \dots, f_k(\cdot))^T$ , that is, for which holds  $\arg \max_c f_c(x) = y$ . We consider the most common

attack-form where an attack aims at misclassification of  $x$  by allowing for some predefined maximum magnitude of perturbation. That is, the attacker targets the optimization problem

$$\begin{aligned} & \text{maximize} \quad \mathcal{L}(f(x + \delta), y) \quad , \\ & \text{subject to} \quad \|\delta\|_p \leq \eta \quad , \end{aligned} \quad (3)$$

where  $\mathcal{L}(\cdot, \cdot)$  is the loss function,  $\|\cdot\|_p$  with  $p \geq 1$  is the  $p$ -norm, and  $\eta$  is the *perturbation strength*, i.e. the maximal allowed magnitude of the attack. Common choices of loss functions are for example cross-entropy and the negative margin  $\mathcal{L}_{\text{margin}}(f(x + \delta), y) = -(f_y(x + \delta) - \max_{c \neq y} f_c(x + \delta))$ . In the case of a *targeted attack* aiming at incorrectly classifying  $x$  as belonging to class  $j$  the loss can be changed to  $-\mathcal{L}(f(x + \delta), j)$ .

From the view of a defender one can wonder if the magnitude of the attack is large enough to lead to a misclassification, i.e., if  $\eta$  is bigger than the minimal perturbation  $\epsilon$  that leads to a misclassification (see figure 1a) for an illustration). In case of linear discriminant functions the minimal distance  $\epsilon$  is given by:

$$\frac{f_y(x) - \max_{c \neq y} f_c(x)}{\|\nabla_x(f_y(x) - \max_{c \neq y} f_c(x))\|_2} \quad . \quad (4)$$

In practice targeting the optimization problem in eq. (3) usually involves estimating  $\delta$  by performing some kind of gradient based optimization on the loss function [e.g. Goodfellow et al., 2015, Madry et al., 2018]. If  $f(\cdot)$  is a stochastic classifier as introduced in the previous subsection the gradient with respect to the input is

$$\nabla_x \mathcal{L}(f^{\mathcal{S}}(x), y) = \mathcal{L}\left(\frac{1}{S} \sum_{s=1}^S f(x, \theta_s), y\right)$$

and thus stochastic as well.

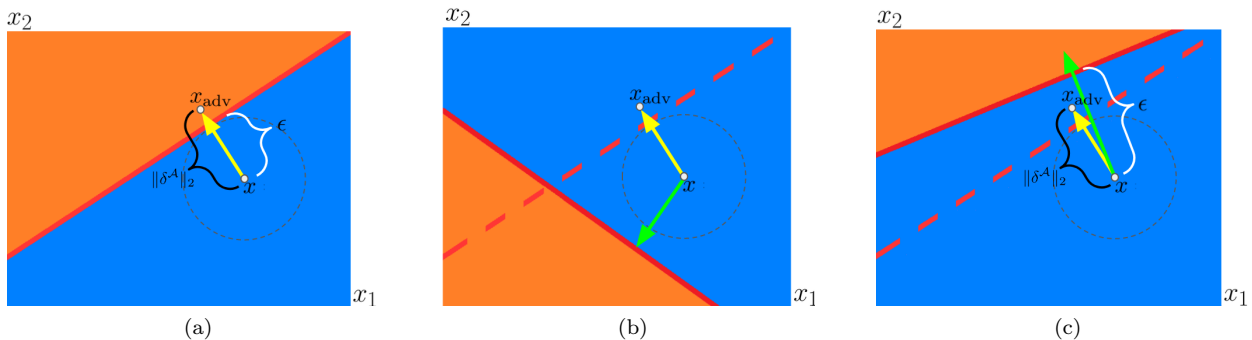


Figure 1: Unsuccessful attacks on a binary stochastic classifier with linear decision boundary. a)  $\epsilon$  is the minimal distance to the decision boundary used for calculating the attack, thus  $x + \delta^{\mathcal{A}}$  can only be an adversarial example if  $\|\delta^{\mathcal{A}}\|_2 \geq \epsilon$  holds. b) and c) show the stochastic decision boundary during attack (dashed) and inference (solid). The green arrows indicate the shortest direction to the latter, respectively. In b)  $\delta^{\mathcal{A}}$  moves  $x$  even further away from the decision boundary used during inference, while in c) the magnitude of  $\delta^{\mathcal{A}}$  is too short to result in an successful attack.

### 3.3 Condition for robustness against gradient based stochastic attacks

In the following we assume that we conduct a gradient based attack and that eq. (1) is not tractable and hence we have to use its MC approximation. This already leads to the “crux” of stochastic classifiers: Each time we calculate a prediction another set of parameters is drawn resulting in another set of discriminant functions and corresponding decision boundaries. To put it into other words, the classifier gets a random variable itself. As a consequence, when calculating a gradient based adversarial attack for an input  $x$  (in a white box-setting) this is done with respect to a drawn set of parameters  $\mathcal{A} = \{\theta_1^a, \theta_2^a, \dots, \theta_{S_{\mathcal{A}}}^a\}$ , and thus  $\delta_{\mathcal{A}}$  from eq. (3) is specific for a realization  $f^{\mathcal{A}}(x)$  of the classifier. During inference, the resulting adversarial example  $x_{\text{adv}} = x + \delta^{\mathcal{A}}$ , is then fed to another random classifier  $f^{\mathcal{I}}$  which is based on a different set of parameters  $\mathcal{I} = \{\theta_1^i, \theta_2^i, \dots, \theta_{S_{\mathcal{I}}}^i\}$ . From this perspective, the prediction network  $f^{\mathcal{I}}$  is robust against the attack, if the distance from  $x$  to the decision boundary given by  $f_y^{\mathcal{I}}(x) - \max_{c \neq y} f_c^{\mathcal{I}}(x) = 0$  in *direction of  $\delta^{\mathcal{A}}$*  is larger than the length of  $\delta^{\mathcal{A}}$ , as illustrated in figure 1b) and c). To turn this line of thoughts into a theorem we first assume the discriminant functions to be linear and derive a sufficient and necessary condition for the prediction network to be robust against the given attack.

**Theorem 3.2** (Sufficient and necessary robustness condition for linear classifiers). *Let  $f : \mathbb{R}^d \times \Omega^h \rightarrow \mathbb{R}^k$  be a stochastic classifier with linear discriminant functions and  $f^{\mathcal{A}}$  and  $f^{\mathcal{I}}$  be two MC estimates of the prediction. Let  $x \in \mathbb{R}^d$  be a data point with label  $y \in [1, \dots, k]$  and  $\arg \max_c f_c^{\mathcal{A}}(x) = \arg \max_c f_c^{\mathcal{I}}(x) = y$ , and let  $x_{adv} = x + \delta^{\mathcal{A}}$  be an adversarial example computed for solving the minimization problem (3) for  $f^{\mathcal{A}}$ . It holds that  $\arg \max_c f_c^{\mathcal{I}}(x + \delta^{\mathcal{A}}) = y$  if and only if*

$$\min_c \tilde{r}_c^{\mathcal{I}} > \|\delta^{\mathcal{A}}\|_2, \quad (5)$$

with

$$\tilde{r}_c^{\mathcal{I}} = \begin{cases} \infty & , \text{ if } \cos(\alpha_c^{\mathcal{I}, \mathcal{A}}) \geq 0 \\ -\frac{f_y^{\mathcal{I}}(x) - f_c^{\mathcal{I}}(x)}{\|\nabla_x(f_y^{\mathcal{I}}(x) - f_c^{\mathcal{I}}(x))\|_2 \cdot \cos(\alpha_c^{\mathcal{I}, \mathcal{A}})} & , \text{ else} \end{cases}$$

and

$$\cos(\alpha_c^{\mathcal{I}, \mathcal{A}}) = \frac{\langle \nabla_x(f_y^{\mathcal{I}}(x) - f_c^{\mathcal{I}}(x)), \delta^{\mathcal{A}} \rangle}{\|\nabla_x(f_y^{\mathcal{I}}(x) - f_c^{\mathcal{I}}(x))\|_2 \cdot \|\delta^{\mathcal{A}}\|_2}.$$

The proof is given in appendix A. The conditions on  $\cos(\alpha_c^{\mathcal{I}, \mathcal{A}})$  have a nice geometrical interpretation. An angle of less than  $90^\circ$  (which corresponds to a positive cosine value) indicates that  $\nabla_x(f_y^{\mathcal{I}}(x) - f_c^{\mathcal{I}}(x))$  and  $\delta^{\mathcal{A}}$  point into “opposite” directions and thus even for infinite long moves into the direction of  $\delta^{\mathcal{A}}$  the label of  $x$  will not be changed to class  $c$ . Note the similarity of  $\tilde{r}_c^{\mathcal{I}}$  to eq. (4). If  $\cos(\alpha_c^{\mathcal{I}, \mathcal{A}}) = -1$  then the SNN is as robust as a corresponding deterministic network. However, if  $\cos(\alpha_c^{\mathcal{I}, \mathcal{A}}) > -1$  the stochastic classifier above is always more robust than its deterministic counterpart. The derived conditions may locally hold for classifiers which can be reasonably well approximated by a first-order Taylor approximation. To derive further guarantees, we can relax the linearity assumption by assuming discriminant functions which are  $L$ -smooth as defined in the following.

**Definition 3.3** ( $L$ -smoothness). A differentiable function  $f : \mathbb{R}^d \rightarrow \mathbb{R}^k$  is  $L$ -smooth, if for any  $x_1, x_2 \in \mathbb{R}^d$  and any output dimension  $c \in [1, \dots, k]$ :

$$\frac{\|\nabla_{x_1} f(x_1)_c - \nabla_{x_2} f(x_2)_c\|_2}{\|x_1 - x_2\|_2} \leq L.$$

For such smooth discriminant function we can derive a sufficient (but not necessary) robustness condition specified by the following theorem which is proven in appendix A.

**Theorem 3.4** (Sufficient condition for the robustness of a  $L$ -smooth stochastic classifier). *In the setting of theorem 3.2 let  $f^{\mathcal{A}}$  and  $f^{\mathcal{I}}$  be instead of linear discriminant functions be  $L$ -smooth discriminant functions. Then it holds that  $\arg \max_c f_c^{\mathcal{I}}(x + \delta^{\mathcal{A}}) = y$  if  $\min_c r_c^{\mathcal{I}} > \|\delta^{\mathcal{A}}\|_2$  with*

$$r_c^{\mathcal{I}} = \begin{cases} \infty & , \text{ if } V \geq 0 \\ \frac{f_y^{\mathcal{I}}(x) - f_c^{\mathcal{I}}(x)}{|V|} & , \text{ else} \end{cases} \quad (6)$$

with  $V = \|\nabla_x(f_y^{\mathcal{I}}(x) - f_c^{\mathcal{I}}(x))\|_2 \cdot \cos(\alpha_c^{\mathcal{I}, \mathcal{A}}) - L \cdot \|\delta^{\mathcal{A}}\|_2$  and  $\cos(\alpha_c^{\mathcal{I}, \mathcal{A}})$  as in theorem 3.2.

For targeted attacks with target class  $j$ , the inequality (5) and its analogue in theorem 3.4 can be simply replaced by  $\tilde{r}_j^{\mathcal{I}} > \|\delta^{\mathcal{A}}\|_2$ .

### 3.4 Robustness of stochastic classifiers

Since in practice neither the parameter set  $\mathcal{A}$  nor  $\mathcal{I}$  is fixed, the quantity really describing the robustness of a stochastic classifier with linear discriminant functions is

$$\mathbb{P}(\min_c \tilde{r}_c^{\mathcal{I}} > \|\delta^{\mathcal{A}}\|_2), \quad (7)$$

where  $\tilde{r}_c^{\mathcal{I}}$  and  $\delta^{\mathcal{A}}$  are random variables. For  $L$ -smooth models, replacing  $\tilde{r}_c^{\mathcal{I}}$  by  $r_c^{\mathcal{I}}$  leads to a lower bound of this probability. Deriving an analytic expression for this probability is a hard problem. However, based on theorem 3.4 (or its analogue for linear discriminant functions) it becomes clear that a larger  $\min_c r_c^{\mathcal{I}}$  and a smaller  $\|\delta^{\mathcal{A}}\|_2$  relate to increasing the probability in eq. (7) and thus to an increased robustness. We note that  $r_c^{\mathcal{I}}$  grows with i) larger prediction margins  $f_y^{\mathcal{I}}(x) - f_c^{\mathcal{I}}(x)$ , ii) smaller gradient norms  $\|\nabla_x(f_y^{\mathcal{I}}(x) - f_c^{\mathcal{I}}(x))\|_2$ , and iii) smaller angles  $\alpha_c^{\mathcal{I}, \mathcal{A}}$ . Further,  $\|\delta^{\mathcal{A}}\|_2$  decreases if the maximal attack length  $\eta$  in the optimization problem in eq. (3) is not exhausted. This provides us with the insights which factors positively impact the robustness of stochastic classifiers. We will discuss these factors, where we will use  $f_{y-c}(x, \cdot) := f_y(x, \cdot) - f_c(x, \cdot)$  to simply notation, in the following.

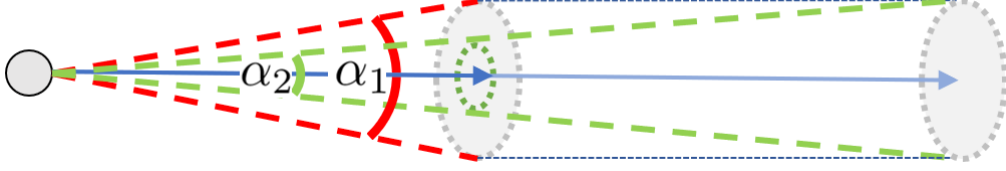


Figure 2: The arrows illustrate the mean  $\nu$  of the gradient in a shorter (dark blue) and longer version (lighter blue). The circles indicate areas of high probability under  $\mathcal{N}(0, \frac{\Xi}{S^I})$  for different covariance magnitudes (gray for larger and green for smaller magnitude). For small mean and small variance the maximal angle that we might observe when sampling  $\epsilon$  and  $\hat{\epsilon}$  from these regions is  $\alpha_2$ . An increase of the covariance results in a larger maximal angle  $\alpha_1$ . When keeping the variance fixed, the maximal angle between samples is larger when the mean is shorter.

**Margin** Recall that the sample-based prediction margin of stochastic classifiers is an approximation of the expected prediction margin given by

$$\mathbb{E}_{p(\Theta)}[f_{y-c}(x, \Theta)] \approx \frac{1}{S^I} \sum_{s=1}^{S^I} f_{y-c}(x, \theta_s^i) .$$

The higher the expected prediction margin the more robust the model. Moreover, as follows from the CLT the variance of the estimate increases with higher prediction variance and decreases with growing sample size  $S^I$ . Since deviations from the expected value are symmetric, they can increase or decrease the robustness.

**Gradient norm** In this paragraph we analyze the norm of the gradient  $f_{y-c}^I(x)$ . To do so, we make use of the following proposition.

**Proposition 3.5.** *Let  $X$  be a random vector following a multivariate normal distribution with mean value  $\mu$  and diagonal covariance matrix  $\Sigma$ . Then the expectation of  $\|X\|_2$  can be upper and lower bounded by*

$$\|\mu\|_2 < \mathbb{E}[\|X\|_2] < \sqrt{\|\mu\|_2^2 + \text{tr}(\Sigma)} .$$

The proof is given in the appendix. To apply proposition 3.5 to the gradient norm, we first rewrite the gradients as

$$\nabla_x f_{y-c}^I(x) = \nabla_x \left( \frac{1}{S^I} \sum_{s=1}^{S^I} f_{y-c}(x, \theta_s^i) \right) .$$

From CLT follows that for sufficiently many samples  $\nabla_x f_{y-c}^I(x) \sim \mathcal{N}(\nu, \frac{\Xi}{S^I})$ . Plugging this into proposition 3.5 yields

$$\|\nu\|_2 \leq \mathbb{E}[\|\nabla_x f_{y-c}^I(x)\|_2] \leq \sqrt{\|\nu\|_2^2 + \text{tr}\left(\frac{\Xi}{S^I}\right)} .$$

With  $\text{tr}\left(\frac{\Xi}{S^I}\right) \xrightarrow{S^I \rightarrow \infty} 0$ , the lower bound is approached. Therefore, the interval in which  $\mathbb{E}[\|\nabla_x(f_{y-c}^I(x) - f_c^I(x))\|_2]$  lies decreases with increased sample size. This fits our assumption that the expected norm decreases with growing sample size and is in general larger for larger  $\Xi$ .

**Angle** Recall, that  $\alpha_c^{I, \mathcal{A}}$  is the angle between two sample based estimators: on the one hand  $\nabla_x f_{y-c}^I(x)$  that is approximately  $\mathcal{N}(\nu, \frac{\Xi}{S^I})$  distributed as discussed in the previous paragraph, and on the other hand  $\delta^{\mathcal{A}}$ . The distribution of  $\delta^{\mathcal{A}}$  depends on which attack is employed. For simplicity let us assume here that the attack is based on a single gradient estimation, that is  $\delta^{\mathcal{A}} = -\nabla_x f_{y-c}^{\mathcal{A}}(x)$ . Let us further assume that we used the same amount of samples during attack as during inference, i.e.  $S^I = S^{\mathcal{A}}$ . Then  $-\delta^{\mathcal{A}}$  is approximately Gaussian distributed as well. Therefore, we can set  $\nabla_x f_{y-c}^I(x) = \nu + \epsilon$  and  $-\delta^{\mathcal{A}} = \nu + \hat{\epsilon}$ , where  $\epsilon, \hat{\epsilon} \sim \mathcal{N}(0, \frac{\Xi}{S^I})$ .

In figure 2 we sketched means of different length as arrows and the regions of high probability of Gaussian's with different covariance as circle. Samples  $\epsilon$  and  $\hat{\epsilon}$  from these regions can lead to maximal angles between the corresponding samples of  $\nabla_x f_{y-c}^I(x)$  and  $-\delta^{\mathcal{A}}$  indicated by the angles between the dashed arrows. Smaller  $\frac{\Xi}{S^I}$  results in smaller expected angles (green compared to red) between  $\nabla_x f_{y-c}^I(x)$  and  $-\delta^{\mathcal{A}}$ , and thus for the angle  $\alpha_c^{I, \mathcal{A}}$  between  $\nabla_x f_{y-c}^I(x)$  and  $\delta^{\mathcal{A}}$  into smaller  $\cos(\alpha_c^{I, \mathcal{A}})$ , which increases the denominator in  $\tilde{r}_c^I$  and hence

reduces the robustness. A larger mean gradient leads to smaller  $\cos(\alpha_c^{\mathcal{I}, \mathcal{A}})$  as well. This leads to the conclusion, that a larger gradient variance (induced by a larger prediction variance), a smaller mean gradient, and a smaller number of samples might increase the robustness of stochastic classifiers.

**Attack length** For a maximal magnitude attack, as defined in (3), it usually holds that  $\|\delta^{\mathcal{A}}\|_p = \eta$ . However, there are some cases where the maximal allowed perturbation is not obtained, i.e.  $\|\delta^{\mathcal{A}}\|_p < \eta$ . This can happen, if the perturbation shifts some entries of  $x$  out of the predefined input space and hence the corresponding entries of  $x + \delta^{\mathcal{A}}$  are “clipped” which reduces  $\|\delta^{\mathcal{A}}\|_p$ . Second,  $\delta^{\mathcal{A}}$  is usually estimated by ascending the loss gradient (or the gradient of a related function) with respect to the inputs in some way. Consequently, no changes occur when the gradient is zero. This happens if the softmax is used in the output layer and if there exists a class  $c$  for which  $f_c(x, \theta_s) = 1$ . In these cases the derivative of the softmax is zero, which leads to a zero gradient. This can be circumvented by conducting attacks based on the logits which we discuss in appendix C.3.

## 4 Experimental robustness analysis

In the following we give a brief explanation of the general data sets and architectures used. We then show how an accuracy based on theorem 3.2 and 3.4 performs compared to the actual observed accuracy under attack. In the three consecutive sections we analyze first the relation between prediction variance and robustness, second the impact of multiple samples during the attack and conclude with discussing the effect of the sample size used during inference.

**Experimental setup** Our experiments are conducted on two kind of architectures: For experiments on the FashionMNIST [Xiao et al., 2017] data set we used feedforward neural networks with two stochastic hidden layers, each with 128 neurons, and a matrix variate normal distribution placed over the weights. We trained these models either as a Variational Matrix Gaussian (VMG, the BNN proposed by Louizos and Welling [2016]) via variational inference, or as an infinite mixture (IM) with the maximum likelihood objective proposed by Däubener and Fischer [2020], which was reported to result in a stochastic model with an increased prediction variance compared to the VMG. For experiments on CIFAR10 [Krizhevsky et al.] we trained two wide residual networks (ResNet) with MC dropout layers [Gal and Ghahramani, 2016] applied after the convolution blocks<sup>1</sup> and dropout probabilities  $p = 0.3$  and  $p = 0.6$ . If not specified otherwise we used 100 samples of  $\Theta$  for inference on both datasets. Further details on how we trained the models can be found in appendix B. Adversarial attacks were calculated with the fast gradient (sign) method (FGM) [Goodfellow et al., 2015],  $L_2$ -norm constraint, and varying perturbation strengths and amounts of samples. The implementation is based on the CleverHans repository [Papernot et al., 2018].

### 4.1 Accuracy of robustness conditions

To investigate the practical transferability of the derived theorems 3.2 and 3.4 we first need to construct an  $L$ -smooth classifier. This can be done based on findings of Salman et al. [2019] and Yang et al. [2022], who derived upper bounds on the  $L$ -smoothness parameter for smoothed classifiers  $g : x \rightarrow \mathbb{E}_\epsilon[f(x + \epsilon)]$ , with  $\epsilon \sim \mathcal{N}(0, \sigma^2)$ . The bound of the latter is given by  $L = 2/\sigma^2$ . Leveraging this insight about smoothed classifiers, we applied randomized smoothing during training by replacing each image in the batch by two noisy copies with Gaussian noise  $\epsilon \sim \mathcal{N}(0, 0.1)$  for the models trained on FashionMNIST and  $\epsilon \sim \mathcal{N}(0, 0.01)$  for models trained on CIFAR10. This ensures  $L \leq 20$  and  $L \leq 200$ , respectively. During prediction we estimated the expectation under the Gaussian noise with 10 (IM and BNN) or 5 (ResNet) samples. We had to reduce the inference sample size to 50 for the ResNets to fit them on one single NVIDIA GeForce RTX 2080 Ti. Note that only the models in the experiment described in this section are trained with randomized smoothing. For calculating the FGM attacks we used 10 samples for all models. We estimated the percentage of resulting attacks for which  $\min_c r_c^{\mathcal{I}} > \|\delta^{\mathcal{A}}\|_2$  and  $\min_c \tilde{r}_c^{\mathcal{I}} > \|\delta^{\mathcal{A}}\|_2$  and compared this to the adversarial accuracy (i.e. the percentage of perturbed samples classified correctly) in figures 3 and figure 8 in appendix C.1. The percentage of samples fulfilling the condition  $\min_c r_c^{\mathcal{I}} > \|\delta^{\mathcal{A}}\|_2$  approaches zero with growing perturbation strength, indicating that the lower bound provided by  $r_c^{\mathcal{I}}$  is rather loose. On the other hand the percentage of samples for which (5) is fulfilled is a quite good approximation of the real accuracy for small attack length, which suggests that the decision boundaries are approximately linear in a small neighborhood of the input.

<sup>1</sup>We used the Pytorch implementation of the model proposed by Zagoruyko and Komodakis [2017] provided by <https://github.com/meliketoy/wide-resnet.pytorch>.



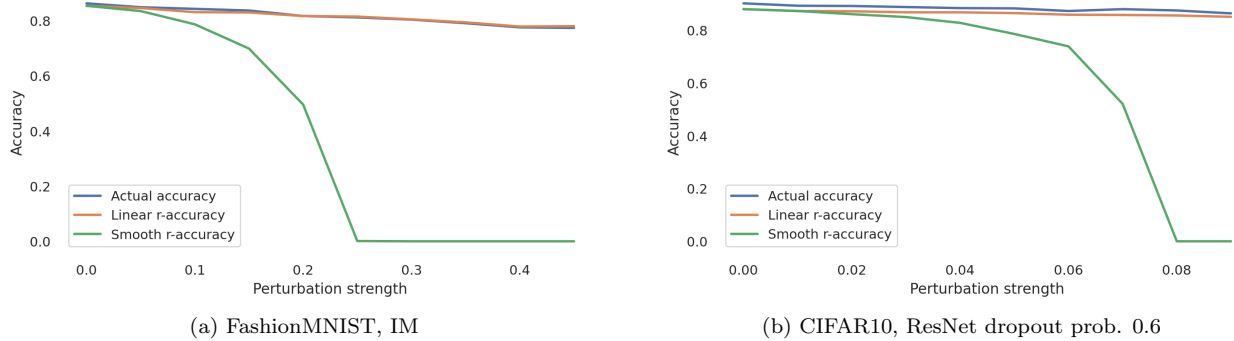


Figure 3: Adversarial accuracy of the smoothed models for attacks based on 10 samples vs percentage of images with  $\min_c r_c^T > \|\delta^A\|_2$  (smooth) and  $\min_c r_c^T > \|\delta^A\|_2$  (linear) for the first 1,000 images from the respective test sets.

## 4.2 Prediction variance as robustness indicator

In this section we compare the properties of SNNs that have the same network architecture and a similar training procedure but different prediction variances. On the one hand we compare the BNN against the IM and on the other we compare the two ResNets with different dropout probabilities against each other. First, we estimated the prediction variance of these models by calculating the empirical variance estimates of  $f_y(x, \Theta)$ , i.e.  $\frac{1}{1000} \sum_{s=1}^{1000} \left( f_y(x, \theta_s) - \frac{1}{1000} \sum_{j=1}^{1000} f_y(x, \theta_j) \right)^2$ , based on the first 1,000 examples from the respective test sets. The results are shown in figure 4. As expected, the IM has a significantly larger prediction variance than the BNN and the prediction variance of the ResNet with higher dropout probability is larger than that with the lower. We then investigated the adversarial robustness of the architectures for different perturbation strength when using 100 samples during inference, shown in figure 5. While model accuracy is similar on clean data (c.f. table 2), models with higher prediction variance were significantly more robust under attack. This can be explained by the fact, that a higher prediction variance leads to smaller angles between the attack direction and the margin gradient, as can be seen by comparing the outer box-plots in figures 6 and 10.

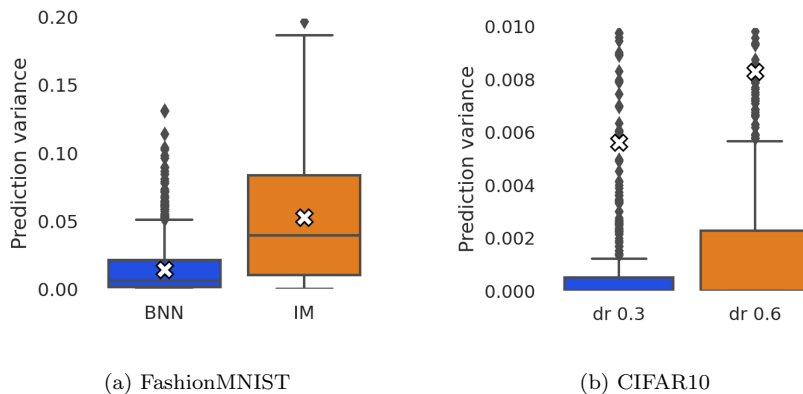


Figure 4: Box plots of the empirical prediction variances (based on 1,000 samples) for the first 1,000 test images. White crosses indicate mean values.

## 4.3 Stronger attacks by increased sample size

In this section we investigate the effect of varying the amount of samples used for calculating the attack, e.g. for  $S^A \in \{1, 5, 10, 100, (1000)\}$ . Figure 5 shows the resulting adversarial robustness of the IM and the ResNet with dropout probability 0.6. The results for the BNN and ResNet with a smaller dropout probability are shown in appendix C.2 figure 9. The accuracy under attack clearly decreases for all models with increasing amount of samples used for calculating the attack. The same holds true if the attacks are calculated based on the FGSM (with  $L_\infty$  constraint) or projected gradient decent [Madry et al., 2018], as shown in appendix C.2. For ResNet we additionally calculated the adversarial robustness when dropout is turned off during inference which turns the model into a deterministic version of itself. The results show that the deterministic network is

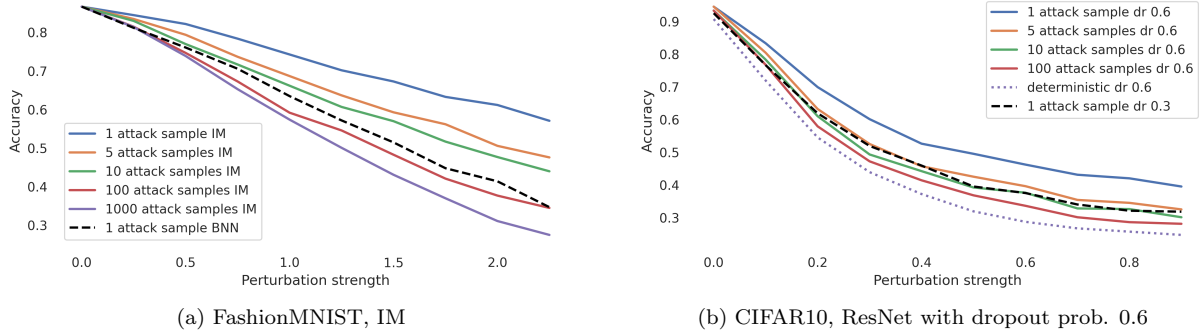


Figure 5: Accuracy under attack for different perturbation strength and amount of samples used for calculating the attack. The dashed line shows the adversarial accuracy for the models with the same architecture but less prediction variance.

less robust than the stochastic ResNet under a strong attack with 100 samples. This is in line with what we would suspect from our theory. Note, that in the linear case the minimal distance to the decision boundary of a deterministic classifier is given by eq. (4) which lacks the  $\cos(\alpha_c^{\mathcal{I},\mathcal{A}})$  term in comparison with  $\tilde{r}_c^{\mathcal{I}}$ . Moreover, even if the attack on SNNs was based on infinitely many samples, it almost never holds that  $\cos(\alpha_c^{\mathcal{I},\mathcal{A}}) = -1$  (which would correspond to the equality of the directions of  $-\delta^{\mathcal{A}}$  and the gradient) because of the stochasticity of the inference procedure, which makes SNNs more robust than their deterministic counterparts.

When estimating the adversarial accuracy we simultaneously analyzed the corresponding values of  $\cos(\alpha_j^{\mathcal{I},\mathcal{A}})$  for the  $j$  with minimal  $\tilde{r}_j^{\mathcal{I}}$  as shown in figure 6 (and figure 10 in appendix C.2). The cosine values are decreasing with growing sample size. This means that when taking more samples during the attack the direction of  $-\delta^{\mathcal{A}}$  is more aligned with  $\nabla_x f_{y-c}^{\mathcal{I}}(x)$ . Moreover, there seems to be a correlation between the cosine values and the network robustness, e.g. a larger number of samples during attack results in larger angles and smaller adversarial accuracies. This observation is in accordance to our theoretical analysis which predicts that an increased amount of samples leads to smaller cosine values and in turn to less adversarial robustness.

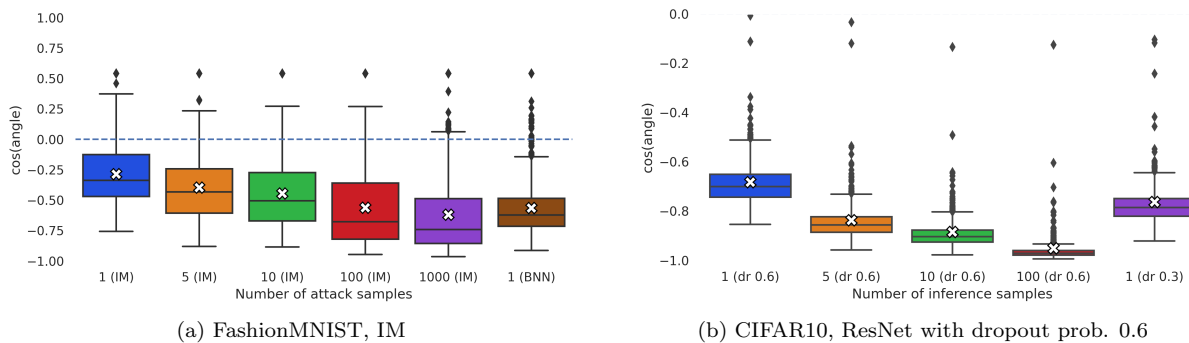


Figure 6: Cosine of the angle for the first 1,000 images from the test sets when attacked with different amounts of samples. White crosses indicate mean values.

#### 4.4 Extreme prediction values and the attack length

In the following we investigate if and which factors discussed in paragraph “Attack length” in section 3.4 are present in our experiments. Therefore, we analyzed in how many cases we observe absolute certain predictions when conducting inference on a single sample, e.g. predictions with  $\max_c f_c(x, \theta) = 1$  which lead to zero gradients. We estimated the amount of such predictions for the 10,000 test set samples of FashionMNIST and CIFAR10. While (n)one are observed for ResNet, we found 397 for the BNN and 2,187 (i.e. for more than every 5-th example!) for the IM. This indicates that higher prediction variance might more often lead to extreme predictions. These vanishing gradients implicitly increase the adversarial accuracy as they decrease the efficient sample size used during the attack. Moreover, they have an impact on the gap between actual attack length and the maximal possible attack length, as shown in table 1. The effect however is reduced by increasing the sample size during attack. Vanishing gradients can be avoided by applying attacks to the logits (for the cost of loosing the correct gradient information), which we found to be beneficial for attacking the IM but not the



Table 1: Average attack length used for attacks with allowed attack length  $\eta = 1.5$  for BNN and IM trained on FashionMNIST, and  $\eta = 0.3$  for ResNets trained on CIFAR10.

SAMPLES	1	5	10	100	1,000
BNN	1.273	1.310	1.317	1.315	1.310
IM	1.035	1.175	1.208	1.264	1.295
DROPOUT 0.3	0.299	0.299	0.299	0.299	-
DROPOUT 0.6	0.299	0.299	0.299	0.299	-

BNN, as we show in appendix C.3.

#### 4.5 Robustness in dependence of the amount of samples used during inference

In practice the amount of samples  $S^{\mathcal{I}}$  drawn during inference is fixed to an arbitrary number. In this section we investigate the impact of varying  $S^{\mathcal{I}} \in \{1, 5, 10, 100\}$  which are values frequently used in practice. We first observe, that only few samples are necessary to get reliable predictions on clean data for all models as shown by the test accuracies in table 2. One could suspect that taking fewer samples during inference might be beneficial for an increased accuracy under attack because of the higher stochasticity. However, we found no significant difference when inference is conducted with at least 5 inference samples (c.f. appendix C.4, figure 17).

Table 2: Test set accuracy with increasing number of samples used during prediction. FashionMNIST: BNN and IM, CIFAR10: ResNet with different dropout probabilities.

SAMPLES	1	5	10	100
BNN	83.16	84.92	85.09	85.20
IM	79.22	84.42	85.18	85.79
DROPOUT 0.3	91.90	92.62	92.71	92.72
DROPOUT 0.6	92.46	93.50	93.55	93.66

To get a better understanding why increasing the stochasticity does not relate to an increased robustness, we analyzed the angle and gradient norm for the first 1,000 test set images for the IM trained on FashionMNIST (results for the other models can be found in appendix C.4). For each image we estimated an one-sample attack with perturbation strength  $\eta = 1.5$  and calculated the angle between  $\delta^{\mathcal{A}}$  and  $\nabla_x \min_c f_{y-c}^{\mathcal{I}}(x)$  for varying  $S^{\mathcal{I}}$ . We observe a similar behavior of  $\cos(\alpha^{\mathcal{I},\mathcal{A}})$  as observed when increasing the attack strength: the angle is increasing and hence the cosine is decreasing with increasing numbers of inference samples (c.f. figure 16 in appendix C.4). Another factor which is influenced by the stochasticity is the gradient norm. From figure 7 a) we see that the mean and the variance of the gradient norm decreases with increasing sample size. This finding supports our conjecture in paragraph ‘‘Gradient norm’’ in section 3.4 that the expected length of the gradient is decreasing when taking more samples during inference. The denominator of eq. (5) corresponds to the product of cosine and the gradient norm, which we depicted in figure 7 b) and which does not change significantly for more than 5 inference samples. Thus, the advantage brought by having a higher stochasticity when using less samples during inference is balanced by the disadvantage of a larger gradient norm, leading to a vanishing effect of the inference sample size on the robustness.

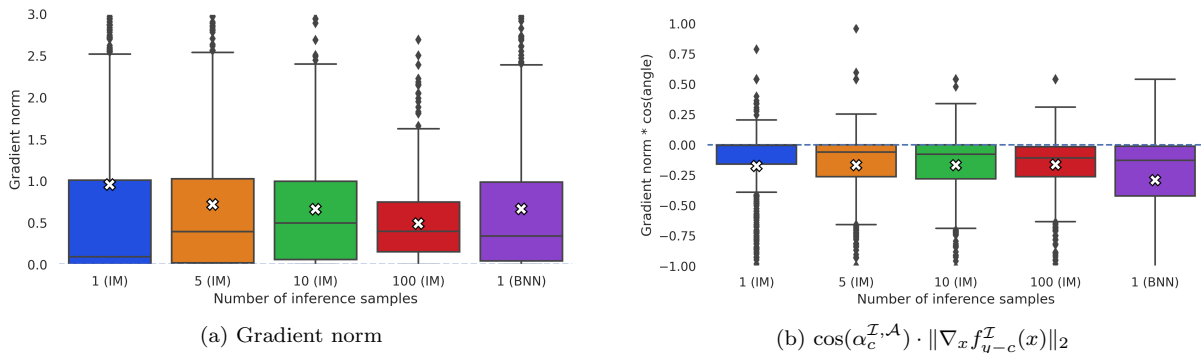


Figure 7: a) Norm of the gradient of the margin during inference and b) cosine of the angle times gradient norm based on different amounts of samples for IM trained on FashionMNIST.

## 5 Conclusion

In this work we have stressed the fact that stochastic neural networks (SNNs) (and stochastic classifiers in general) depend on samples and are thus random variables themselves. For gradient-based adversarial attacks this means that the attack is calculated based on one realization of the stochastic net (which depends on multiple samples from the random variables used in the network) and applied to another which is used for inference. We derived a sufficient condition for this inference network to be robust against the calculated attack. This allowed us to identify the factors that lead to an increased robustness of stochastic classifiers: i) larger prediction margins ii) a higher angle between the attack direction and the direction to the closest decision boundary during inference, iii) a smaller gradient norm, and iv) a reduced attack length. We showed that all these factors depend on the prediction variance and the amount of samples used for attack estimation and inference. This insight allows us to explain why SNNs are more robust than deterministic nets, why more samples increase the attack strength, why the number of samples used during inference has no significant effect on robustness, and why higher prediction variances translate to robuster SNNs. These findings stress the importance of analyzing the impact of the sample sizes used when comparing the adversarial robustness of SNNs and will help the development of more robust SNNs in future.

## Acknowledgment

This work was funded by the Deutsche Forschungsgemeinschaft (DFG, German Research Foundation) under Germany's Excellence Strategy - EXC 2092 CASA - 390781972.

## References

- Sravanti Addepalli, Samyak Jain, Gaurang Sriramanan, and R. Venkatesh Babu. Boosting adversarial robustness using feature level stochastic smoothing. In *Proceedings of the IEEE/CVF Conference on Computer Vision and Pattern Recognition (CVPR) Workshops*, pages 93–102, June 2021.
- Naveed Akhtar and Ajmal Mian. Threat of adversarial attacks on deep learning in computer vision: A survey. *IEEE Access*, 6:14410–14430, 2018. doi: 10.1109/ACCESS.2018.2807385.
- Anish Athalye, Nicholas Carlini, and David A. Wagner. Obfuscated gradients give a false sense of security: Circumventing defenses to adversarial examples. In *Proceedings of the 35th International Conference on Machine Learning (ICML)*, pages 274–283, 2018. URL <http://proceedings.mlr.press/v80/athalye18a.html>.
- Christopher Bender, Yang Li, Yifeng Shi, Michael K. Reiter, and Junier Oliva. Defense through diverse directions. In *Proceedings of the 37th International Conference on Machine Learning (ICML)*, pages 756–766, 2020.
- Battista Biggio, Iginio Corona, Davide Maiorca, Blaine Nelson, Nedim Šrndić, Pavel Laskov, Giorgio Giacinto, and Fabio Roli. Evasion attacks against machine learning at test time. In Hendrik Blockeel, Kristian Kersting, Siegfried Nijssen, and Filip Železný, editors, *Machine Learning and Knowledge Discovery in Databases*, pages 387–402. Springer Berlin Heidelberg, 2013. ISBN 978-3-642-40994-3.
- Sébastien Bubeck. Convex optimization: Algorithms and complexity. In *arXiv preprint <https://arxiv.org/pdf/1405.4980>*, 2015.
- Ginevra Carbone, Matthew Wicker, Luca Laurenti, Andrea Patane', Luca Bortolussi, and Guido Sanguinetti. Robustness of bayesian neural networks to gradient-based attacks. In *Advances in Neural Information Processing Systems (NeurIPS)*, volume 33, pages 15602–15613, 2020.
- Nicholas Carlini and David Wagner. Towards evaluating the robustness of neural networks. In *IEEE Symposium on Security and Privacy (SP)*, pages 39–57, 2017a.
- Nicholas Carlini and David Wagner. *Adversarial Examples Are Not Easily Detected: Bypassing Ten Detection Methods*, page 3–14. Association for Computing Machinery, 2017b. ISBN 9781450352024.
- Nicholas Carlini, Guy Katz, Clark Barrett, and David L. Dill. Provably minimally-distorted adversarial examples. In *arXiv preprint <https://arxiv.org/abs/1709.10207>*, 2018.
- Jeremy Cohen, Elan Rosenfeld, and Zico Kolter. Certified adversarial robustness via randomized smoothing. In *Proceedings of the 36th International Conference on Machine Learning (ICML)*, volume 97, pages 1310–1320. PMLR, 2019.

- Francesco Croce and Matthias Hein. Provable robustness against all adversarial  $l_p$ -perturbations for  $p \geq 1$ . In *International Conference on Learning Representations (ICLR)*, 2020.
- Francesco Croce, Maksym Andriushchenko, and Matthias Hein. Provable robustness of relu networks via maximization of linear regions. In *Proceedings of the Twenty-Second International Conference on Artificial Intelligence and Statistics*, volume 89, pages 2057–2066. PMLR, 2019.
- Ali Dabouei, Sobhan Soleymani, Fariborz Taherkhani, Jeremy Dawson, and Nasser M. Nasrabadi. Exploiting joint robustness to adversarial perturbations. In *IEEE/CVF Conference on Computer Vision and Pattern Recognition (CVPR)*, pages 1119–1128, 2020. doi: 10.1109/CVPR42600.2020.00120.
- Guneet S. Dhillon, Kamyar Azizzadenesheli, Jeremy D. Bernstein, Jean Kossaifi, Aran Khanna, Zachary C. Lipton, and Animashree Anandkumar. Stochastic activation pruning for robust adversarial defense. In *International Conference on Learning Representations (ICLR)*, 2018.
- Sina Däubener and Asja Fischer. Investigating maximum likelihood based training of infinite mixtures for uncertainty quantification. In *arXiv preprint <https://arxiv.org/abs/2008.03209>*, 2020.
- Yarin Gal and Zoubin Ghahramani. Dropout as a bayesian approximation: Representing model uncertainty in deep learning. In *Proceedings of The 33rd International Conference on Machine Learning (ICML)*, volume 48, pages 1050–1059. PMLR, 2016.
- Ian J. Goodfellow, Jonathon Shlens, and Christian Szegedy. Explaining and harnessing adversarial examples. In *3rd International Conference on Learning Representations, (ICLR)*, 2015.
- Zhezhi He, Adnan Siraj Rakin, and Deliang Fan. Parametric noise injection: Trainable randomness to improve deep neural network robustness against adversarial attack. In *Proceedings of the IEEE/CVF Conference on Computer Vision and Pattern Recognition (CVPR)*, 2019.
- Matthias Hein and Maksym Andriushchenko. Formal guarantees on the robustness of a classifier against adversarial manipulation. In *Advances in Neural Information Processing Systems (NeurIPS)*, volume 30. Curran Associates, Inc., 2017.
- Andrew Ilyas, Shibani Santurkar, Dimitris Tsipras, Logan Engstrom, Brandon Tran, and Aleksander Madry. Adversarial examples are not bugs, they are features. In *Advances in Neural Information Processing Systems (NeurIPS)*, volume 32. Curran Associates, Inc., 2019.
- Guy Katz, Clark Barrett, David L. Dill, Kyle Julian, and Mykel J. Kochenderfer. Reluplex: An efficient smt solver for verifying deep neural networks. In *Computer Aided Verification*, pages 97–117. Springer International Publishing, 2017. ISBN 978-3-319-63387-9.
- Diederik P. Kingma and Jimmy Ba. Adam: A method for stochastic optimization. In *3rd International Conference on Learning Representations (ICLR)*, 2015.
- Alex Krizhevsky, Vinod Nair, and Geoffrey Hinton. Cifar-10 (canadian institute for advanced research). In <http://www.cs.toronto.edu/~kriz/cifar.html>.
- Mathias Lécyer, Vaggelis Atlidakis, Roxana Geambasu, Daniel Hsu, and Suman Jana. Certified robustness to adversarial examples with differential privacy. In *IEEE Symposium on Security and Privacy (SP)*, pages 656–672. IEEE, 2019.
- Christos Louizos and Max Welling. Structured and efficient variational deep learning with matrix gaussian posteriors. In *Proceedings of The 33rd International Conference on Machine Learning (ICML)*, volume 48, pages 1708–1716. PMLR, 2016.
- Aleksander Madry, Aleksandar Makelov, Ludwig Schmidt, Dimitris Tsipras, and Adrian Vladu. Towards deep learning models resistant to adversarial attacks. In *International Conference on Learning Representations (ICLR)*, 2018.
- Radford M. Neal. *Bayesian Learning for Neural Networks*. Springer-Verlag, Berlin, Heidelberg, 1996. ISBN 0387947248.
- Nicolas Papernot, Patrick McDaniel, Xi Wu, Somesh Jha, and Ananthram Swami. Distillation as a defense to adversarial perturbations against deep neural networks. In *IEEE Symposium on Security and Privacy (SP)*, pages 582–597, 2016. doi: 10.1109/SP.2016.41.

- Nicolas Papernot, Fartash Faghri, Nicholas Carlini, Ian Goodfellow, Reuben Feinman, Alexey Kurakin, Cihang Xie, Yash Sharma, Tom Brown, Aurko Roy, Alexander Matyasko, Vahid Behzadan, Karen Hambardzumyan, Zhishuai Zhang, Yi-Lin Juang, Zhi Li, Ryan Sheatsley, Abhibhav Garg, Jonathan Uesato, Willi Gierke, Yinpeng Dong, David Berthelot, Paul Hendricks, Jonas Rauber, and Rujun Long. Technical report on the cleverhans v2.1.0 adversarial examples library. In *arXiv preprint <https://arxiv.org/abs/1610.00768>*, 2018.
- Edward Raff, Jared Sylvester, Steven Forsyth, and Mark McLean. Barrage of random transforms for adversarially robust defense. In *IEEE/CVF Conference on Computer Vision and Pattern Recognition (CVPR)*, pages 6521–6530, 2019. doi: 10.1109/CVPR.2019.00669.
- Hadi Salman, Jerry Li, Ilya Razenshteyn, Pengchuan Zhang, Huan Zhang, Sebastien Bubeck, and Greg Yang. Provably robust deep learning via adversarially trained smoothed classifiers. In *Advances in Neural Information Processing Systems (NeurIPS)*, volume 32. Curran Associates, Inc., 2019.
- Christian Szegedy, Wojciech Zaremba, Ilya Sutskever, Joan Bruna, Dumitru Erhan, Ian J. Goodfellow, and Rob Fergus. Intriguing properties of neural networks. In *2nd International Conference on Learning Representations (ICLR)*, 2014.
- Jonathan Uesato, Brendan O’Donoghue, Pushmeet Kohli, and Aäron van den Oord. Adversarial risk and the dangers of evaluating against weak attacks. In *Proceedings of the 35th International Conference on Machine Learning (ICML)*, volume 80, pages 5032–5041. PMLR, 2018.
- Matthew Wicker, Luca Laurenti, Andrea Patane, and Marta Kwiatkowska. Probabilistic safety for bayesian neural networks. In *Proceedings of the Thirty-Sixth Conference on Uncertainty in Artificial Intelligence, UAI*, volume 124 of *Proceedings of Machine Learning Research*, pages 1198–1207. AUAI Press, 2020.
- Matthew Wicker, Luca Laurenti, Andrea Patane, Zhuotong Chen, Zheng Zhang, and Marta Kwiatkowska. Bayesian inference with certifiable adversarial robustness. In *Proceedings of The 24th International Conference on Artificial Intelligence and Statistics*, volume 130, pages 2431–2439. PMLR, 2021.
- Eric Wong and J. Zico Kolter. Provable defenses against adversarial examples via the convex outer adversarial polytope. In *Proceedings of the 35th International Conference on Machine Learning (ICML)*, volume 80, pages 5283–5292. PMLR, 2018.
- Han Xiao, Kashif Rasul, and Roland Vollgraf. Fashion-mnist: a novel image dataset for benchmarking machine learning algorithms. In *arXiv preprint <https://arxiv.org/abs/1708.07747>*, 2017.
- Cihang Xie, Jianyu Wang, Zhishuai Zhang, Zhou Ren, and Alan Yuille. Mitigating adversarial effects through randomization. In *International Conference on Learning Representations (ICLR)*, 2018.
- Zhuolin Yang, Linyi Li, Xiaojun Xu, Bhavya Kailkhura, Tao Xie, and Bo Li. On the certified robustness for ensemble models and beyond. In *International Conference on Learning Representations (ICLR)*, 2022.
- Sergey Zagoruyko and Nikos Komodakis. Wide residual networks. In *arXiv preprint <https://arxiv.org/abs/1605.07146>*, 2017.

## A Proofs

We start by restating and proving the theorem in the case of linear discriminant function:

**Theorem A.1** (Sufficient and necessary robustness condition for linear classifiers). *Let  $f : \mathbb{R}^d \times \Omega^h \rightarrow \mathbb{R}^k$  be a stochastic classifier with linear discriminant functions and  $f^{\mathcal{A}}$  and  $f^{\mathcal{I}}$  be two MC estimates of the prediction. Let  $x \in \mathbb{R}^d$  be a data point with label  $y \in [1, \dots, k]$  and  $\arg \max_c f_c^{\mathcal{A}}(x) = \arg \max_c f_c^{\mathcal{I}}(x) = y$ , and let  $x_{adv} = x + \delta^{\mathcal{A}}$  be an adversarial example computed for solving the minimization problem (3) for  $f^{\mathcal{A}}$ . It holds that  $\arg \max_c f_c^{\mathcal{I}}(x + \delta^{\mathcal{A}}) = y$  if and only if*

$$\min_c \tilde{r}_c^{\mathcal{I}} > \|\delta^{\mathcal{A}}\|_2, \quad (8)$$

with

$$\tilde{r}_c^{\mathcal{I}} = \begin{cases} \infty & , \text{ if } \cos(\alpha_c^{\mathcal{I},\mathcal{A}}) \geq 0 \\ -\frac{f_y^{\mathcal{I}}(x) - f_c^{\mathcal{I}}(x)}{\|\nabla_x(f_y^{\mathcal{I}}(x) - f_c^{\mathcal{I}}(x))\|_2 \cdot \cos(\alpha_c^{\mathcal{I},\mathcal{A}})} & , \text{ else} \end{cases}$$

and

$$\cos(\alpha_c^{\mathcal{I},\mathcal{A}}) = \frac{\langle \nabla_x(f_y^{\mathcal{I}}(x) - f_c^{\mathcal{I}}(x)), \delta^{\mathcal{A}} \rangle}{\|\nabla_x(f_y^{\mathcal{I}}(x) - f_c^{\mathcal{I}}(x))\|_2 \cdot \|\delta^{\mathcal{A}}\|_2}.$$

*Proof.* An adversarial attack on  $f^{\mathcal{I}}$  with the adversarial example  $x + \delta^{\mathcal{A}}$  is not successful iff  $\forall c \in \{1, 2, \dots, k\}, c \neq y$ :

$$f_y^{\mathcal{I}}(x + \delta^{\mathcal{A}}) - f_c^{\mathcal{I}}(x + \delta^{\mathcal{A}}) > 0.$$

With a Taylor expansion around  $x$  we can rewrite  $f_y^{\mathcal{I}}(x + \delta^{\mathcal{A}}) - f_c^{\mathcal{I}}(x + \delta^{\mathcal{A}})$  as

$$\begin{aligned} & f_y^{\mathcal{I}}(x) + \langle \nabla_x f_y^{\mathcal{I}}(x), \delta^{\mathcal{A}} \rangle - f_c^{\mathcal{I}}(x) - \langle \nabla_x f_c^{\mathcal{I}}(x), \delta^{\mathcal{A}} \rangle \\ &= f_y^{\mathcal{I}}(x) - f_c^{\mathcal{I}}(x) + \langle \nabla_x f_y^{\mathcal{I}}(x) - \nabla_x f_c^{\mathcal{I}}(x), \delta^{\mathcal{A}} \rangle \\ &= f_y^{\mathcal{I}}(x) - f_c^{\mathcal{I}}(x) + \|\nabla_x(f_y^{\mathcal{I}}(x) - f_c^{\mathcal{I}}(x))\|_2 \cdot \|\delta^{\mathcal{A}}\|_2 \cdot \cos(\alpha_c^{\mathcal{I},\mathcal{A}}) \end{aligned} \quad (9)$$

where  $\alpha_c^{\mathcal{I},\mathcal{A}} := \angle(\nabla_x(f_y^{\mathcal{I}}(x) - f_c^{\mathcal{I}}(x)), \delta^{\mathcal{A}})$ . We can distinguish two cases for each  $c$ .

**Case 1:**  $\cos(\alpha_c^{\mathcal{I},\mathcal{A}}) \geq 0$ . In this case last term of eq. (9) is positive or zero and thus

$$f_y^{\mathcal{I}}(x + \delta^{\mathcal{A}}) - f_c^{\mathcal{I}}(x + \delta^{\mathcal{A}}) \geq f_y^{\mathcal{I}}(x) - f_c^{\mathcal{I}}(x) > 0,$$

where the second inequality holds since  $\arg \max_c f_c^{\mathcal{I}}(x) = y$ .

**Case 2:**  $\cos(\alpha_c^{\mathcal{I},\mathcal{A}}) < 0$ . In this case the last term of equation eq. (9) is negative and thus

$$f_y^{\mathcal{I}}(x + \delta^{\mathcal{A}}) - f_c^{\mathcal{I}}(x + \delta^{\mathcal{A}}) \leq f_y^{\mathcal{I}}(x) - f_c^{\mathcal{I}}(x).$$

As we see from rearranging eq. (9), it holds  $f_y^{\mathcal{I}}(x + \delta^{\mathcal{A}}) - f_c^{\mathcal{I}}(x + \delta^{\mathcal{A}}) > 0$  if

$$\tilde{r}_c^{\mathcal{I}} := -\frac{f_y^{\mathcal{I}}(x) - f_c^{\mathcal{I}}(x)}{\|\nabla_x(f_y^{\mathcal{I}}(x) - f_c^{\mathcal{I}}(x))\|_2 \cdot \cos(\alpha_c^{\mathcal{I},\mathcal{A}})} > \|\delta^{\mathcal{A}}\|_2. \quad (10)$$

For each class  $c$  either case 1 holds and we define  $\tilde{r}_c^{\mathcal{I}} := \infty$ , or condition (10) needs to be full-filled, which yields the condition stated in the theorem.  $\square$

**Proposition A.2** (Bubeck [2015]). *Let  $f$  be a  $L$ -smooth function on  $\mathbb{R}^n$ . For any  $x, y \in \mathbb{R}^n$  it holds:*

$$|f(y) - f(x) - \langle \nabla_x f(x), y - x \rangle| \leq \frac{L}{2} \|y - x\|_2^2.$$

*Proof.* From the fundamental theorem of calculus we know that for a differentiable function  $f$  it holds that  $f(y) - f(x) = \int_x^y \nabla_t f(t) dt$ . By substituting  $x_t = x + t(y - x)$  we see that  $x_0 = x$  and  $x_1 = y$  and thus we can

write  $f(y) - f(x) = \int_0^1 \nabla f(x + t(y-x))^T \cdot (y-x) dt$ . This allows the following approximations

$$\begin{aligned}
& |f(y) - f(x) - \langle \nabla_x f(x), y-x \rangle| \\
&= \left| \int_0^1 \nabla f(x + t(y-x))^T \cdot (y-x) dt - (\nabla_x f(x))^T (y-x) \right| \\
&\leq \int_0^1 |(\nabla f(x + t(y-x)) - \nabla_x f(x))^T \cdot (y-x)| dt \\
&\stackrel{\text{Cauchy-Schwarz}}{\leq} \int_0^1 \|\nabla f(x + t(y-x)) - \nabla_x f(x)\|_2 \cdot \|y-x\|_2 dt \\
&\stackrel{L\text{-smoothness}}{\leq} L \cdot \|y-x\|_2^2 \cdot \int_0^1 t dt \\
&= \frac{L}{2} \cdot \|y-x\|_2^2 .
\end{aligned}$$

□

**Theorem A.3** (Sufficient condition for the robustness of a L-smooth stochastic classifier). *Let  $f : \mathbb{R}^d \times \Omega^h \rightarrow \mathbb{R}^k$  be a stochastic classifier with L-smooth discriminant functions and  $f^{\mathcal{A}}$  and  $f^{\mathcal{I}}$  be two MC estimates of the prediction. Let  $x \in \mathbb{R}^d$  be a data point with label  $y \in [1, \dots, k]$  and  $\arg \max_c f_c^{\mathcal{A}}(x) = \arg \max_c f_c^{\mathcal{I}}(x) = y$ , and let  $x_{adv} = x + \delta^{\mathcal{A}}$  be an adversarial example computed for solving the minimization problem (3) for  $f^{\mathcal{A}}$ . It holds that  $\arg \max_c f_c^{\mathcal{I}}(x + \delta^{\mathcal{A}}) = y$  if*

$$\min_c r_c^{\mathcal{I}} > \|\delta^{\mathcal{A}}\|_2 ,$$

with

$$r_c^{\mathcal{I}} = \begin{cases} \infty & , \text{ if } \|\nabla_x (f_y^{\mathcal{I}}(x) - f_c^{\mathcal{I}}(x))\|_2 \cdot \cos(\alpha_c^{\mathcal{I},\mathcal{A}}) - L \cdot \|\delta^{\mathcal{A}}\|_2 \geq 0 \\ \frac{f_y^{\mathcal{I}}(x) - f_c^{\mathcal{I}}(x)}{\|\|\nabla_x (f_y^{\mathcal{I}}(x) - f_c^{\mathcal{I}}(x))\|_2 \cdot \cos(\alpha_c^{\mathcal{I},\mathcal{A}}) - L \cdot \|\delta^{\mathcal{A}}\|_2\|} & , \text{ else} \end{cases}$$

and

$$\cos(\alpha_c^{\mathcal{I},\mathcal{A}}) = \frac{\langle \nabla_x (f_y^{\mathcal{I}}(x) - f_c^{\mathcal{I}}(x)), \delta^{\mathcal{A}} \rangle}{\|\nabla_x (f_y^{\mathcal{I}}(x) - f_c^{\mathcal{I}}(x))\|_2 \cdot \|\delta^{\mathcal{A}}\|_2} .$$

*Proof.* For better readability we write  $f_{y-c}^{\mathcal{I}}(x) := f_y^{\mathcal{I}}(x) - f_c^{\mathcal{I}}(x)$ . Using the result from proposition A.2, we can lower bound  $f_{y-c}^{\mathcal{I}}(x + \delta^{\mathcal{A}})$  by

$$\begin{aligned}
& f_{y-c}^{\mathcal{I}}(x) + \langle \nabla_x (f_{y-c}^{\mathcal{I}}(x)), \delta^{\mathcal{A}} \rangle - L \cdot \|\delta^{\mathcal{A}}\|_2^2 \\
&= f_{y-c}^{\mathcal{I}}(x) + \|\nabla_x f_{y-c}^{\mathcal{I}}(x)\|_2 \cdot \|\delta^{\mathcal{A}}\|_2 \cdot \cos(\alpha_c^{\mathcal{I},\mathcal{A}}) - L \cdot \|\delta^{\mathcal{A}}\|_2^2 \\
&= f_{y-c}^{\mathcal{I}}(x) + (\|\nabla_x f_{y-c}^{\mathcal{I}}(x)\|_2 \cdot \cos(\alpha_c^{\mathcal{I},\mathcal{A}}) - L \cdot \|\delta^{\mathcal{A}}\|_2) \cdot \|\delta^{\mathcal{A}}\|_2 \\
&\leq f_{y-c}^{\mathcal{I}}(x + \delta^{\mathcal{A}}) .
\end{aligned} \tag{11}$$

If eq. (11) is bigger than zero, the attack cannot be successful. Hence,

$$0 \stackrel{!}{<} f_{y-c}^{\mathcal{I}}(x) + \left( \|\nabla_x f_{y-c}^{\mathcal{I}}(x)\|_2 \cdot \cos(\alpha_c^{\mathcal{I},\mathcal{A}}) - L \cdot \|\delta^{\mathcal{A}}\|_2 \right) \cdot \|\delta^{\mathcal{A}}\|_2 \tag{12}$$

$$-f_{y-c}^{\mathcal{I}}(x) < \left( \|\nabla_x f_{y-c}^{\mathcal{I}}(x)\|_2 \cdot \cos(\alpha_c^{\mathcal{I},\mathcal{A}}) - L \cdot \|\delta^{\mathcal{A}}\|_2 \right) \cdot \|\delta^{\mathcal{A}}\|_2 \tag{13}$$

**Case 1:**  $\|\nabla_x f_{y-c}^{\mathcal{I}}(x)\|_2 \cdot \cos(\alpha_c^{\mathcal{I},\mathcal{A}}) - L \cdot \|\delta^{\mathcal{A}}\|_2 < 0$ . Transforming eq. (13) leads to

$$\frac{f_{y-c}^{\mathcal{I}}(x)}{\|\|\nabla_x f_{y-c}^{\mathcal{I}}(x)\|_2 \cdot \cos(\alpha_c^{\mathcal{I},\mathcal{A}}) - L \cdot \|\delta^{\mathcal{A}}\|_2\|} > \|\delta^{\mathcal{A}}\|_2 .$$

**Case 2 :**  $\|\nabla_x f_{y-c}^{\mathcal{I}}(x)\|_2 \cdot \cos(\alpha_c^{\mathcal{I},\mathcal{A}}) - L \cdot \|\delta^{\mathcal{A}}\|_2 = 0$ . In this case eq. (12) is trivially fulfilled because  $0 < f_{y-c}^{\mathcal{I}}(x)$  per definition.



**Case 3:**  $\|\nabla_x f_{y-c}^T(x)\|_2 \cdot \cos(\alpha_c^{T,\mathcal{A}}) - L \cdot \|\delta^{\mathcal{A}}\|_2 > 0$ . For this case we get, that

$$-\frac{f_{y-c}^T(x)}{\|\nabla_x f_{y-c}^T(x)\|_2 \cdot \cos(\alpha_c^{T,\mathcal{A}}) - L \cdot \|\delta^{\mathcal{A}}\|_2} < \|\delta^{\mathcal{A}}\|_2 ,$$

which is always guaranteed based on the initial assumption that the benign input was classified correctly, which concludes the proof.  $\square$

**Proposition A.4.** *Let  $X$  be a  $N$ -dimensional random vector following a multivariate normal distribution with mean vector  $\mu$  and diagonal covariance matrix  $\Sigma$ . Then the expectation of  $\|X\|_2$  can be upper and lower bounded by*

$$\|\mu\|_2 < \mathbb{E}[\|X\|_2] < \sqrt{\|\mu\|_2^2 + \text{tr}(\Sigma)} .$$

*Proof.* We first look at the lower bound which by convexity of the norm and Jensen inequality can be derived via

$$\mathbb{E}[\|X\|_2] > \|\mathbb{E}[X]\|_2 = \|\mu\|_2 .$$

Let  $X' \sim \mathcal{N}(0, \mathbf{1}_N)$ , with  $\mathbf{1}_N$  an  $N$ -dimensional unit matrix. With Jensen inequality and convexity of the square function we derive the upper bound

$$\begin{aligned} \mathbb{E}[\|X\|_2] &= \mathbb{E}[\|\mu + X' \cdot \Sigma^{1/2}\|_2] \\ &\leq \left( \mathbb{E} \left[ \left\| \mu + X' \cdot \Sigma^{1/2} \right\|_2^2 \right] \right)^{1/2} \\ &= \left( \|\mu\|_2^2 + 2\mu^T \Sigma^{1/2} \mathbb{E}[X'] + \mathbb{E} \left[ X'^T \Sigma^{1/2T} \Sigma^{1/2} X' \right] \right)^{1/2} \\ &= \sqrt{\|\mu\|_2^2 + \text{tr}(\Sigma)} . \end{aligned}$$

$\square$

## B Hyperparameter

### B.1 Models trained on FashionMNIST

For training the BNN and IM we used the exact same hyperparameters. First, we assumed a standard normal prior decomposed as matrix variate normal distributions for the BNN and respectively added a Kullback-Leibler distance to a standard matrix variate normal distribution as a regularization for the infinite mixture model. We used the provided training and test data split by torchvision. For both models we used a batch size of 100 and trained for 50 epochs with Adam [Kingma and Ba, 2015] and an initial learning rate of 0.001. To leverage the difference between IM and BNN we used 5 samples to approximate the expectation in the ELBO/IM-objective.

### B.2 Models trained on CIFAR10

As stated in the main part, we used the wide ResNet of depth 28 and widening factor 10 provided by <https://github.com/meliketoy/wide-resnet.pytorch> with dropout probabilities 0.3 and 0.6 and all of their learning hyperparameters which are: training for 200 epochs with batch size 100, stochastic gradient descent as optimizer with momentum 0.9, weight decay 5e-4 and a scheduled learning rate decreasing from an initial 0.1 for epoch 0-60 to 0.02 for 60-120 and lastly 0.004 for epochs 120-200.

## C Additional experimental results

In this section we present the results which were not shown in the main part due to space restrictions.

### C.1 Complementary experiments on accuracy of robustness conditions

For completeness we attached the results on the transferability of our derived sufficient conditions of the two remaining models: the BNN on FashionMNIST and the ResNet with dropout probability 0.3 on CIFAR10. We used the same setting as described in section 4.1 and derive similar results (c.f. figure 8): while the percentage of samples fulfilling the condition  $\min_c r_c^T > \|\delta^{\mathcal{A}}\|_2$  approaches zero with growing perturbation strength the percentage of samples fulfilling condition (8) closely matches the real adversarial accuracy.

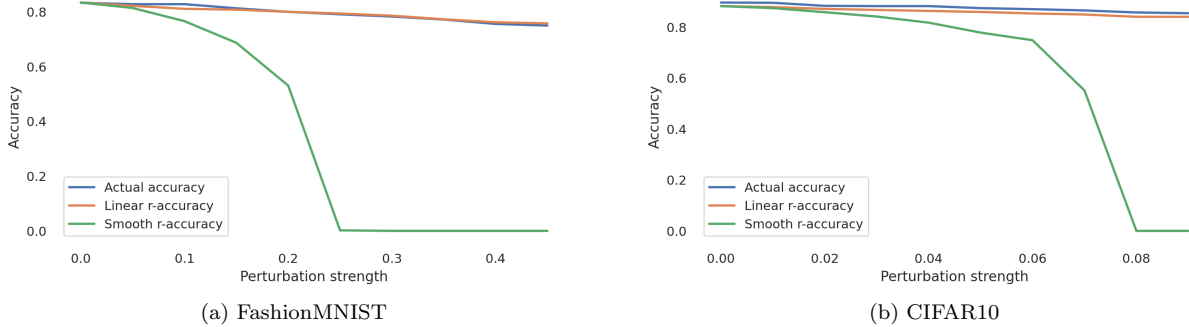


Figure 8: Adversarial accuracy of the a) smoothed BNN and b) smoothed ResNet with dropout probability 0.3 vs percentage of images for which  $\min_c r_c^T > \|\delta^{\mathcal{A}}\|_2$  (smooth) and  $\min_c \tilde{r}_c^T > \|\delta^{\mathcal{A}}\|_2$  (linear) for 1,000 images from the respective test sets. Attacks were conducted on the smoothed classifier with using 10 attack samples.

## C.2 Complementary experiments on stronger attacks by increased sample size

We start this section with the results not shown in the main paper for the adversarial accuracy in dependence of an increased amount of samples during the attack (c.f. figure 9). As previously discussed, the accuracy under attack is reduced by an increased amount of samples during the attack. However, we observe only a very small decrease in accuracy when increasing the amount of samples from 100 and 1,000 for the BNN and when using 5 instead of 10 or 100 samples for the attack on the ResNet trained with dropout probability 0.3. This observation is in line with the quick reduction of  $\cos(\alpha_c^{\mathcal{T}, \mathcal{A}})$  displayed in figure 10 where we see very similar cosine boxplots when more samples are used during the attack.

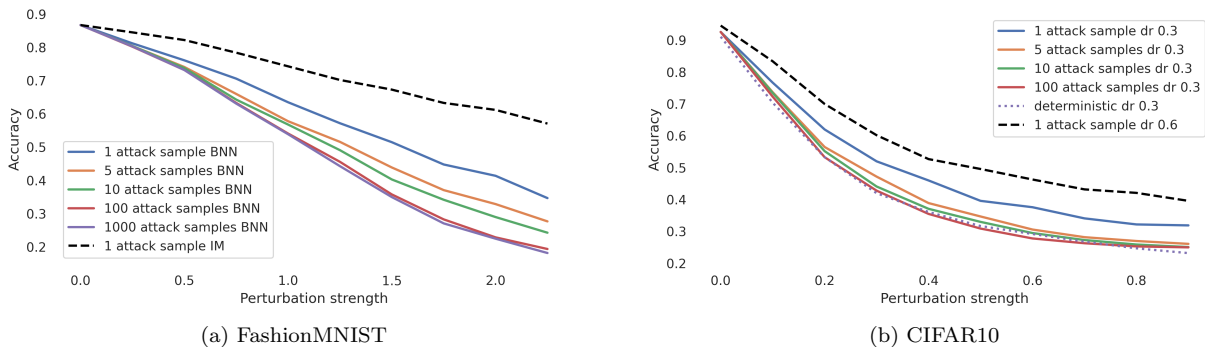


Figure 9: Accuracy under FGM attack for a) the BNN on FashionMNIST and b) ResNet with dropout probability 0.3 on CIFAR10 for different perturbation strengths and amount of samples used for calculating the attack.

**Attacks with FGSM ( $L_\infty$ - norm)** All adversarial examples in the main part of the paper were based on a  $L_2$ -norm constraint, which we chose for the nice geometric distance interpretation. However, the first proposed attack scheme [Goodfellow et al., 2015] was based on  $L_\infty$ -norm, which we test in the following. In figure 11 and 12 we see the respective results on the different data sets. For all models the robustness is decreased with multiple samples and models with higher prediction variance also have a higher accuracy under this attack. Note, that the values of the perturbation strength are not comparable to the values under  $L_2$ - norm constraint, since  $\|x\|_\infty \leq \|x\|_2$ .

**Attacks with PGD** Projected gradient decent [Madry et al., 2018] is a strong iterative attack, where multiple small steps of size  $\nu$  of fast gradient method are applied. Specifically, we used the same  $L_2$ -norm length constraint on  $\eta$  as in the experiments of the main part of the paper but chose step size  $\nu = \eta/5$  and 10 iterations. Note that at each iteration a new network is sampled such that for an attack based on 1 samples, 10 different attack networks were seen, for an attack based on 5 samples 50 different networks and so on. In figure 13 and 14 we see that the overall accuracy is slightly lower than what we have observed with the weaker attack, but still, IM has a higher accuracy under attack than the BNN and so does the ResNet with a higher dropout probability.

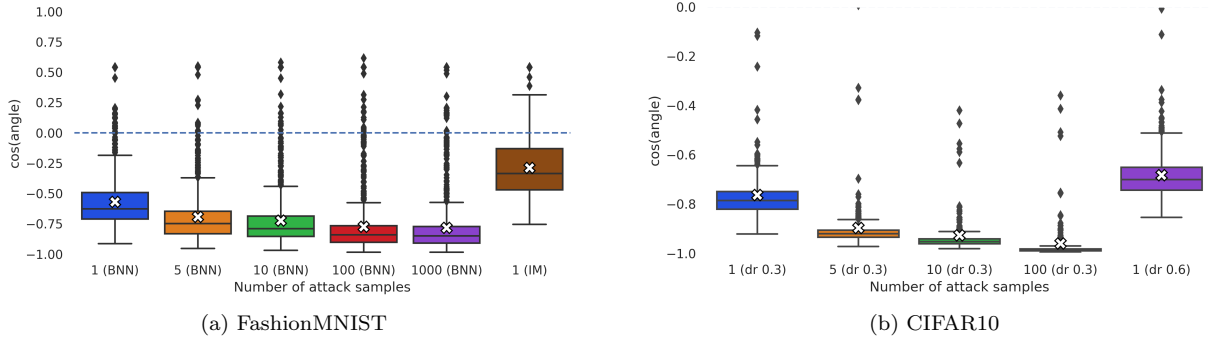


Figure 10: Cosine of the angle for the first 1,000 images from the FashionMNIST and CIFAR10 test set for an a) BNN and b) ResNet trained with dropout probability 0.3 when attacked with different amounts of samples and attack strength 1.5 and 0.3 with FGM respectively. White crosses indicate the mean value.

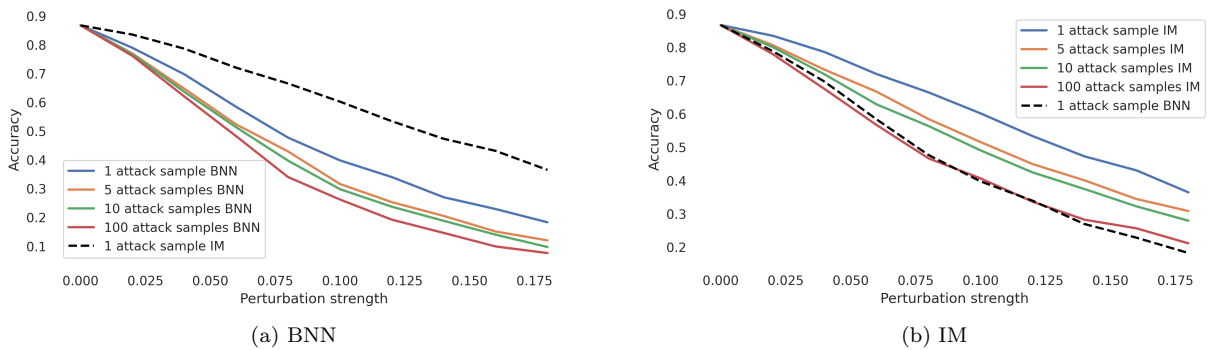


Figure 11: Accuracy under FGSM attack under  $L_\infty$ -norm constraint for a) the BNN and b) the IM on FashionMNIST for different perturbation strengths and amount of samples used for calculating the attack.

### C.3 Complementary experiments on extreme prediction values and the attack length

In section 3.4 we discussed how the attack length might be influenced by zero gradients. A practical solution to circumvent this problem in the case of deterministic networks is to calculate the gradient based on the logits [Carlini and Wagner, 2017a]. This approach is feasible for classifier whose predictions do not depend on the scaling of the output, that is, outputs which are equally expressive in both intervals  $[0, 1]$  and  $[-\infty, \infty]$ . In stochastic networks, where  $f_c(x, \Theta)$  in eq. (1) is per definition a probability like for example in Bayesian neural networks, the shortcut over taking the gradient over logits leads to distorted gradients. For completeness, we nevertheless look at the performance of an attack based on the logits for the two different models trained on FashionMNIST: IM and BNN. We conducted an adversarial attack based on 10 samples, but instead of using the cross-entropy loss we used the Carlini-Wagner (CW) loss [Carlini and Wagner, 2017a] on the averaged logits given by

$$CW(x, \Theta^A) = \max \left( \max_{i \neq t} (Z(x, \Theta^A)_i) - Z(x, \Theta^A)_t, 0 \right),$$

where  $Z(x, \Theta^A)_t = \frac{1}{S^A} \sum_{s=1}^{S^A} Z(x, \theta_s)_t$  is an arbitrary averaged logit of an output node for input  $x$  and parameters  $\theta_s$ . In figure 15 it is shown, that the CW attack on the infinite mixture model improves upon the original attack scheme, whereas it decreases the attack's success for the BNN, where vanishing gradients did not occur that often (c.f. section 4.4). We additionally conducted an attack based on the margin loss  $\mathcal{L}(x + \delta^A, y) = -(\min_c f_{y-c}(x))$  (denoted by the stars), but we found that it performs similar to default cross-entropy loss.

### C.4 Complementary experiments on robustness in dependence of the amount of samples used during inference

In the main part of the paper we argued why, surprisingly, the amount of samples during inference does not influence the robustness, even though we see in figure 16 that less sample lead to the highest values for  $\cos(\alpha^{\mathcal{I}, A})$ . As stated in the main part, the increased gradient norm when using only few samples seems to compensate the

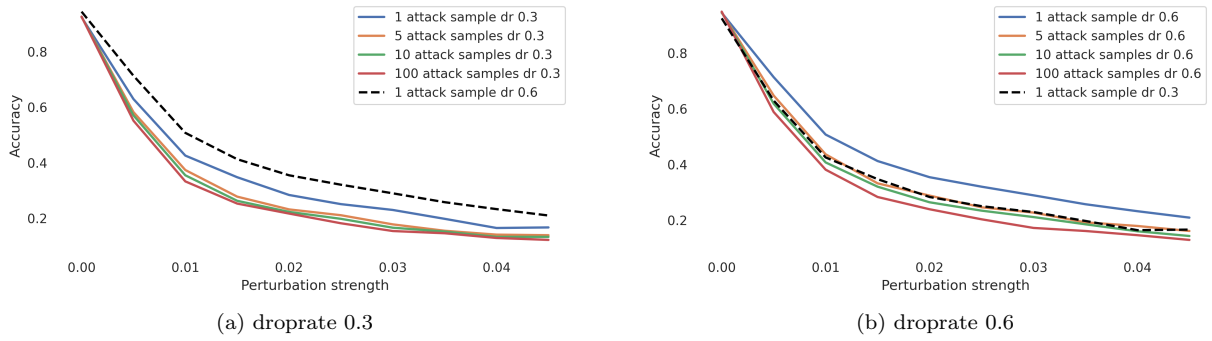


Figure 12: Accuracy under FGSM attack under  $L_\infty$ -norm constraint for the ResNet model with a dropout probability a) of 0.3 and b) of 0.6 on CIFAR10 for different perturbation strengths and amount of samples used for calculating the attack.

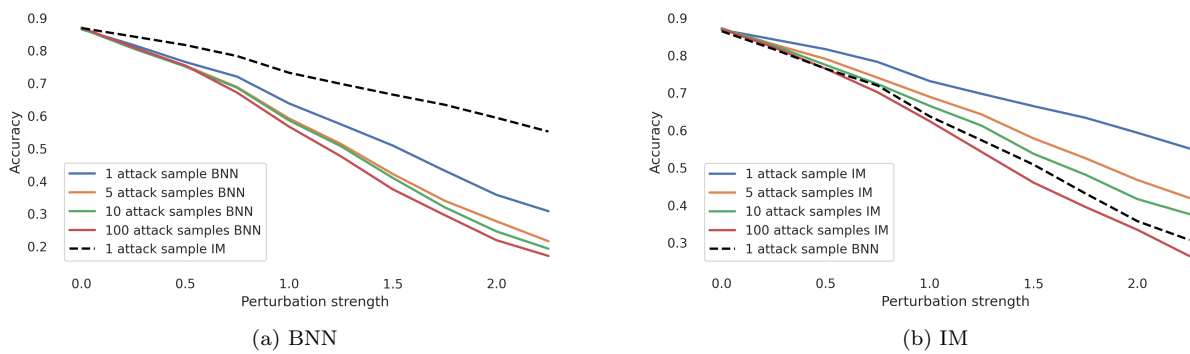


Figure 13: Accuracy under PGD attack for a) the BNN and b) the IM on FashionMNIST for different perturbation strengths and amount of samples used for calculating the attack.

assumed benefits with regard to the angle for using few samples. This can also be seen in figure 17, where a (negative) effect on the robustness can only be observed for one inference sample, which also leads to the worst test set accuracy.

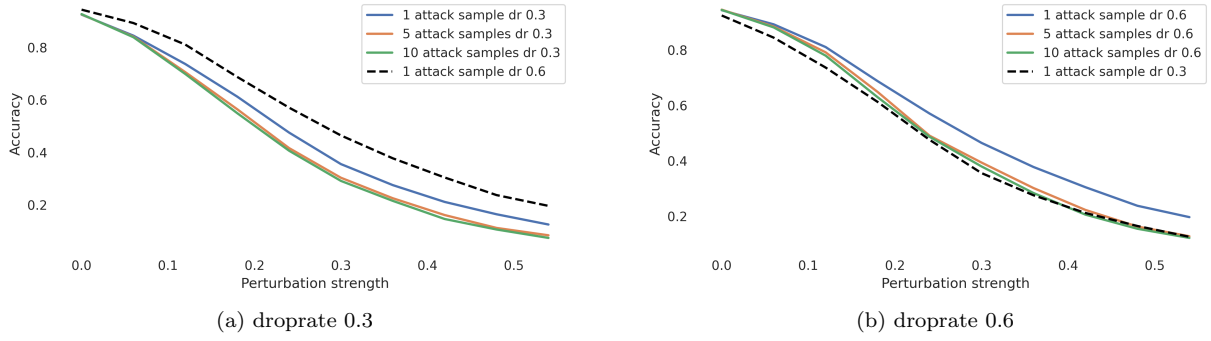


Figure 14: Accuracy under PGD attack for the ResNet with a dropout probability of a) 0.3 and b) of 0.6 on CIFAR10 for different perturbation strengths and amount of samples used for calculating the attack.

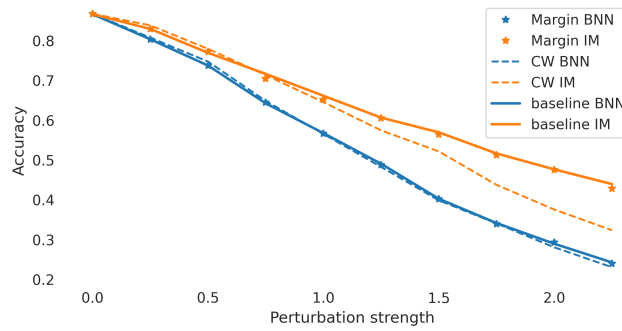


Figure 15: Accuracy under attack with varying perturbation strengths for different attack objectives used for calculating adversarial examples based on one sample for the models trained on FashionMNIST.

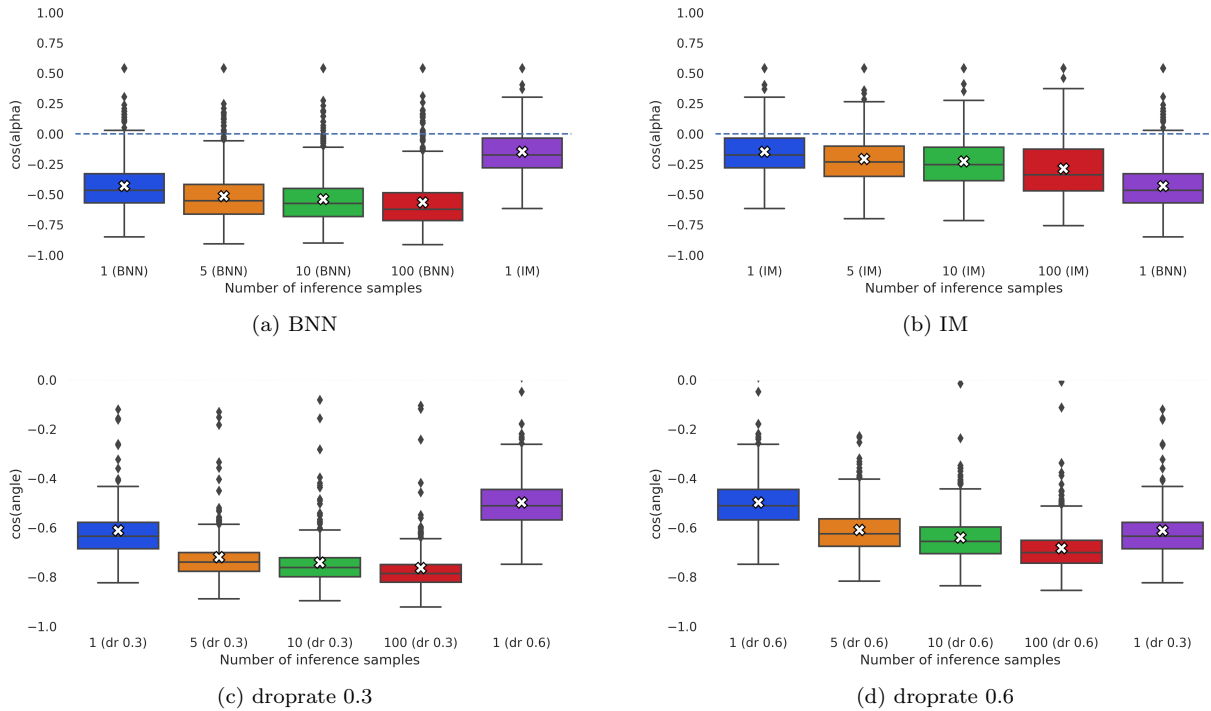
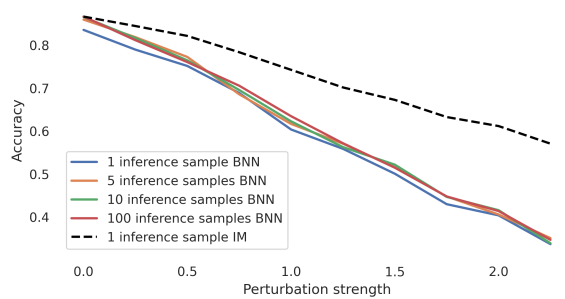
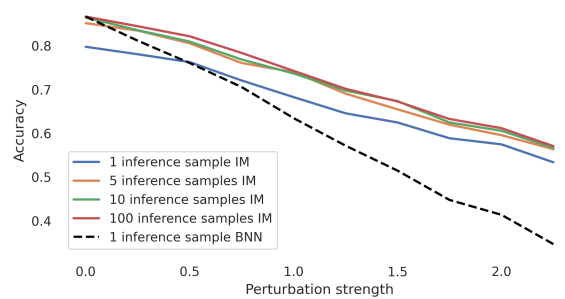


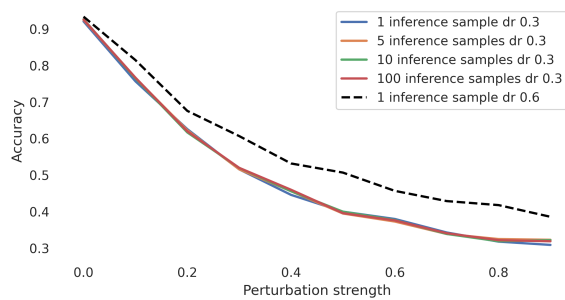
Figure 16: Cosine of the angle for models trained on FashionMNIST ( a and b ) and trained on CIFAR10 ( c and d ) for different amounts of samples used during inference. Used attack direction  $\delta$  was calculated based on 1 sample of FGM under  $L_2$ -norm constraint with  $\eta = 1.5$  and  $0.3$  respectively.



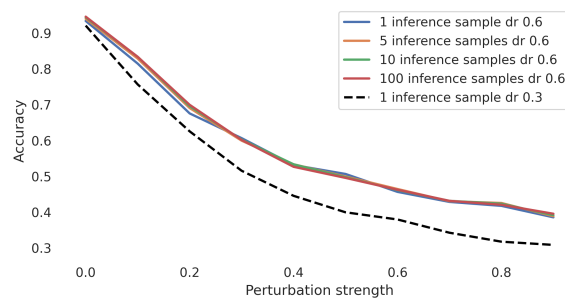
(a) BNN



(b) IM



(c) dropout 0.3



(d) dropout 0.6

Figure 17: Accuracy under attack on a) b) FashionMNIST and c) d) CIFAR10 for different amounts of samples used during inference. Used attack direction  $\delta$  was calculated based on 1 sample of FGM under  $L_2$ -norm and different perturbation strengths.